

**MICROSCOPIC DESCRIPTION OF NUCLEAR
WOBLING MOTION**
— Rotation of triaxially deformed nuclei —

TAKUYA SHOJI and YOSHIFUMI R. SHIMIZU

*Department of Physics, Graduate School of Sciences,
Kyushu University, Fukuoka 812-8581, Japan*

Received (received date)

Revised (revised date)

The nuclear wobbling motion in the Lu region is studied by the microscopic cranked mean-field plus RPA method. The Woods-Saxon potential is used as a mean-field with a new parameterization which gives reliable description of rapidly rotating nuclei. The prescription of symmetry-preserving residual interaction makes the calculation of the RPA step parameter-free, and we find the wobbling-like RPA solution if the triaxial deformation of the mean-field is suitably chosen. It is shown that the calculated out-of-band $B(E2)$ of the wobbling-like solution depends on the triaxial deformation in the same way as in the macroscopic rotor model, and can be used to probe the triaxiality of the nuclear mean-field.

1. Introduction

In this talk we would like to discuss a fundamental question: How nucleus rotates if it is triaxially deformed? Namely, the question is whether nucleus exhibits the so-called wobbling rotational motion. We have been conducting research on this subject for many years, and we would like to report, especially, on the recent development of our microscopic study of the wobbling rotation.

The wobbling motion is an analogy of the quantized motion of the macroscopic (“rigid-body”) triaxial rotor. The spectra of the model hamiltonian of triaxial rotor can be solved approximately (using the $\hbar = 1$ unit) like this;¹

$$H_{\text{rot}} = \frac{I_x^2}{\mathcal{J}_x} + \frac{I_y^2}{\mathcal{J}_y} + \frac{I_z^2}{\mathcal{J}_z}, \Rightarrow E(I, n) \approx \frac{I(I+1)}{2\mathcal{J}_x} + \omega_{\text{wob}}(n+1/2), \quad (1)$$

where the wobbling energy ω_{wob} is given by

$$\omega_{\text{wob}} = \left(\frac{I}{\mathcal{J}_x} \right) \sqrt{\left(\frac{\mathcal{J}_x}{\mathcal{J}_y} - 1 \right) \left(\frac{\mathcal{J}_x}{\mathcal{J}_z} - 1 \right)}. \quad (2)$$

Here it is assumed that the main rotation axis is the x -axis ($\mathcal{J}_x > \mathcal{J}_y, \mathcal{J}_z$). This type of rotational motion is only possible when the system is triaxially deformed, and appears as a multiple band structure shown in Fig. 1. It is composed of a

2 Authors' Names

group of bands lying on top of each other, whose horizontal sequences are usual rotational bands connected by the strong stretched ($|\Delta I| = 2$) $E2$ transitions, while the vertical sequences are connected by slightly weaker $|\Delta I| = 1$ $E2$ transitions. In this way, the vertical excitation, which corresponds to tilting the angular momentum vector (in the body-fixed frame), can be regarded as the phonon-like excitation, $n = 1, 2, \dots$ in Eq. (1), whose phonon energy is given by the famous formula (2).

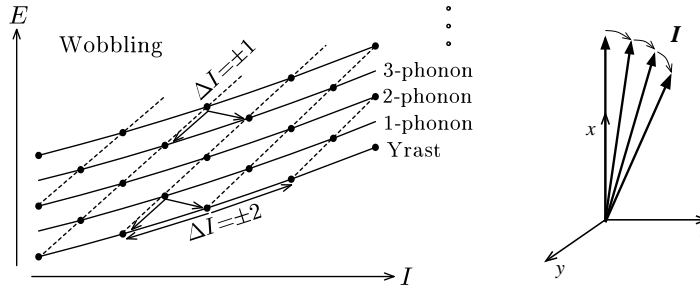


Fig. 1. A schematic illustration of the band structure of the wobbling motion.

Until quite recently, there is no definite evidence of the multiple band structure that exhibits this characteristic feature. It has, however, been first discovered in ^{163}Lu .² The one phonon wobbling band has been measured nowadays in some Lu isotopes,^{3,4,5} and moreover the two phonon wobbling band has been identified in ^{163}Lu .⁶ These bands are examples of the so-called triaxial superdeformed (TSD) bands in the Lu and Hf region. The measured in-band ($\Delta I = -2$) $B(E2)$ values between the horizontal sequences in these TSD bands are typically about 500–700 Weisskopf units, and the out-of-band ($\Delta I = -1$) $B(E2)$ values from the one-phonon wobbling band to the yrast TSD band are about 100 units or more.⁷ These values are very large and consistent to the wobbling picture predicted by the macroscopic particle-rotor model,^{8,9} where an odd $i_{13/2}$ quasiproton is coupled to the rotor.

The triaxial deformation is crucial to realize the wobbling motion. Then, it is important to know how the effects of triaxiality appear in observables. One is the $B(E2)$, which are related to the two intrinsic quadrupole moments, Q_{20} and Q_{22} ,

$$Q_{20} = \sqrt{\frac{5}{16\pi}} \sum_{a=1}^A (2z^2 - x^2 - y^2)_a, \quad Q_{22} = \sqrt{\frac{15}{32\pi}} \sum_{a=1}^A (x^2 - y^2)_a, \quad (3)$$

and the triaxiality parameter γ is defined in terms of them as usual:

$$\tan \gamma = -\frac{\sqrt{2} \langle Q_{22} \rangle}{\langle Q_{20} \rangle} \quad (\text{Lund convention of sign}). \quad (4)$$

The other is the energy spectra, which reflects the properties of the three different moments of inertia about intrinsic axes. Here, it should be pointed out that the characteristic feature of the out-of-band $E2$ transitions observed in Lu nuclei suggests the “positive γ ” shape, i.e. the main rotation axis (the x -axis in our notation)

is the shortest axis in that shape. This shape completely contradicts the well-known irrotational moments of inertia, in which \mathcal{J}_y is the largest, and then the wobbling frequency (2) becomes imaginary. Therefore, we don't know what kind of inertia should be used in macroscopic models, and a microscopic approach is necessary.

2. Microscopic approach

In order to understand the wobbling motion in Lu nuclei, we use a standard microscopic approach; the cranked mean-field and the random phase approximation (RPA). The basic idea is to describe the horizontal rotational bands in Fig. 1 by the semiclassical cranking prescription, and at the same time, the vertical phonon-like excitation in terms of the RPA, which is known to be successful for describing the collective vibrational modes. Namely,

$$h' = h_{\text{def}} - \omega_{\text{rot}} J_x, \quad (\text{cranking}) \quad (5)$$

$$[H', X_n^\dagger] = \omega_n X_n^\dagger, \quad (\text{RPA}) \quad \text{with } H' = h' + V_{\text{int}}, \quad (6)$$

where h_{def} is the triaxially deformed mean-field hamiltonian with the cranking frequency ω_{rot} about the x -axis, X_n^\dagger is the creation operator of the n -th RPA eigen mode with the eigen energy ω_n , and V_{int} is the residual interaction.

It should be emphasized that the residual interaction is constructed so as to restore the rotational symmetry broken by a general mean-field, i.e.

$$[h_{\text{def}}, J_k] \neq 0 \quad \Rightarrow \quad [h_{\text{def}} + V_{\text{int}}, J_k] = 0, \quad (k = x, y, z), \quad (7)$$

with

$$V_{\text{int}} = -\frac{1}{2} \sum_{k=x,y,z} \kappa_k F_k^2, \quad F_k \equiv [h_{\text{def}}, iJ_k], \quad \kappa_k \equiv \langle [[h_{\text{def}}, J_k], J_k] \rangle, \quad (8)$$

where the expectation value is taken with respect to the cranked mean-field yrast state. Thus the RPA solutions are determined without any ambiguities by a given mean-field, and there are no adjustable parameters in the RPA step.

However, it is not clear how the result of such a microscopic approach is related to the wobbling picture of the macroscopic rotor model. It was shown by Marshalek¹⁰ many years ago that, if an appropriate RPA mode exists, the rotor model wobbling picture naturally appears by going from the uniformly rotating (UR) frame, where the cranking prescription is applied, over to the principal axis (PA) frame. Taking into account the fact that the RPA can be regarded as a small amplitude limit of the time-dependent mean-field theory, the time-dependent mean-field describing the wobbling motion is given in the UR frame as

$$h_{\text{UR}}(t) = h_{\text{def}} - \omega_{\text{rot}} J_x - \kappa_y \mathcal{F}_y(t) F_y - \kappa_z \mathcal{F}_z(t) F_z, \quad (9)$$

where $\mathcal{F}_k(t) \equiv \langle F_k \rangle_{\text{UR}}(t)$ ($k = y, z$) are the UR frame expectation values; only the y and z components are relevant to the wobbling phonon excitation, which transfers spin by $\Delta I = \pm 1$. In the case of the harmonic oscillator potential, e.g.

4 Authors' Names

the Nilsson potential, the operators F_y and F_z are proportional to Q_y and Q_z , the non-diagonal quadrupole tensor operators. Even in the case of general potentials, these non-diagonal parts Q_k ($k = x, y, z$) are used to define the PA frame;

$$\langle Q_k \rangle_{\text{PA}} = 0, \text{ (PA condition), } Q_k = \sqrt{\frac{15}{4\pi}} \sum_{a=1}^A (x_i x_j)_a, \text{ (} k, i, j \text{)-cyclic.} \quad (10)$$

The shape fluctuation vanishes by this PA frame condition, but the fluctuation of the angular momentum vector appears in place of it; thus the time-dependent mean-field in the PA frame is transformed as

$$h_{\text{PA}}(t) = h_{\text{def}} - \omega_x(t)J_x - \omega_y(t)J_y - \omega_z(t)J_z, \quad (11)$$

where $\omega_x(t) \approx \omega_{\text{rot}}$ in the small amplitude limit, and the presence of $\omega_y(t)$ and $\omega_z(t)$ reflects that the angular frequency vector also fluctuates about the main rotation axis (the x -axis). The relation between the UR and PA frames is depicted schematically in Fig. 2. The PA frame corresponds to the body-fixed frame of the rotor, and the moments of inertia are naturally introduced by

$$\mathcal{J}_x \equiv \langle J_x \rangle / \omega_{\text{rot}}, \quad \mathcal{J}_y(n) \equiv J_y(n) / \omega_y(n), \quad \mathcal{J}_z(n) \equiv J_z(n) / \omega_z(n), \quad (12)$$

where $J_k(n)$ and $\omega_k(n)$ ($k = y, z$) are Fourier components of the PA frame expectation values with respect to the n -th RPA eigen mode. Using these microscopically calculated moments of inertia, the RPA excitation energy can be written in exactly the same form (2) as in the macroscopic rotor model. It can be also shown¹¹ that the out-of-band $B(E2)$ calculated by the RPA approach can be expressed in the same way as in the rotor model.

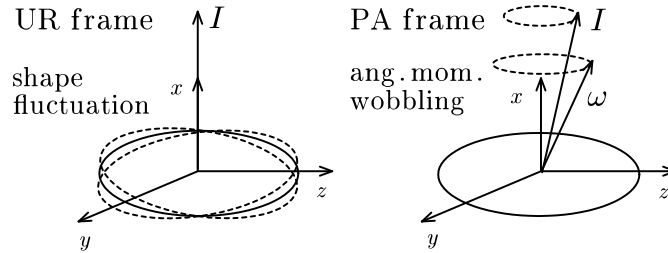


Fig. 2. A schematic illustration depicting the relation between two dynamical pictures in the uniformly rotating (UR) frame and the principal axis (PA) frame.

3. Results of microscopic calculations

Realistic calculations based on the Marshalek's theory have been carried out in the previous works.^{12,11} After the discovery of the wobbling phonon excitation in the TSD bands in the Lu and Hf region, new calculations have been performed, and it is confirmed that the wobbling-like RPA solutions do exist.^{13,14} However, the

Nilsson potential has been used in these calculations, and they are suffered from the problem of large moments of inertia because of the spurious velocity dependence coming from the l^2 -term. Therefore, we have conducted new research with using the Woods-Saxon potential as a nuclear mean-field. Especially, a new parameterization of the Woods-Saxon potential has been provided quite recently by Ramon Wyss, with which it is possible to nicely reproduce the basic properties like the neutron and proton density distributions. This is very important to obtain reliable results for the moments of inertia and the quadrupole moments.

3.1. Mean-field parameters

As it is discussed in the previous section, there is no adjustable parameter in the RPA step once the mean-field is specified. Therefore, let us briefly explain the mean-field parameters used in our calculation. In principle, they should be determined selfconsistently by minimizing the energy. Actually we are developing the Woods-Saxon Strutinsky calculations, but it is not available yet. Therefore we have taken the deformation parameters corresponding to the minimum of the Nilsson Strutinsky calculations, an example of which is shown in Fig. 3. The TSD minimum moves slightly as a function of the rotational frequency but the amount of change is small, so that we have used average values, $\beta_2 = 0.42$, $\gamma = 12^\circ$, $\beta_4 = 0.034$ in all the calculations. we have checked that the qualitative feature of the calculated results does not change if these values are modified in a reasonable range.

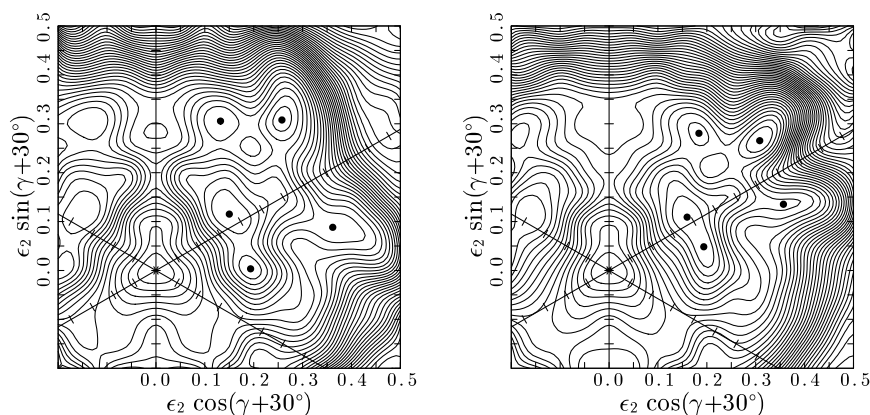


Fig. 3. An example of the potential energy surface obtained by the cranked Nilsson Strutinsky calculation for the $\pi_{i_{13/2}}$ (π, α) = (+, +1/2) configuration at $I = 53/2^+$ in ^{163}Lu . The energy between contours is 250 keV. In the left figure is adopted the “usual” γ , which is used to parameterize the Nilsson potential, while in the right one the calculations are same but the γ defined by a similar Eq. to (4) (see the footnote in the text) is adopted.

Here we would like to point out that there are various different definitions for the triaxiality parameter γ . In this presentation, we use the one defined by Eq. (4) throughout, which is directly related to the two intrinsic quadrupole moments, and

6 Authors' Names

so the $B(E2)$. In Fig. 3, the same calculations are employed but two representations with different definitions of γ are shown. The left part is an usual representation, where the γ is the one used in the Nilsson potential, and the TSD minimum has $\gamma \approx 20^\circ$ and $\epsilon_2 \approx 0.4$. In the right part the definition similar to Eq. (4) is used^a keeping the ϵ_2 as usual, and then the TSD minimum has $\gamma \approx 12^\circ$. Thus, the difference between the two definitions for the same shape is rather large for large ϵ_2 deformation like in the case of the TSD bands. More details about the various definitions of γ parameters and relations between them will be discussed elsewhere.¹⁵

The neutron and proton pairing gaps are also important mean-field parameters. We have used the following parameterization, which is convenient to avoid the abrupt pairing collapse;

$$\Delta(\omega_{\text{rot}}) = \Delta_0 \times \begin{cases} \left[1 - \frac{1}{2} \left(\frac{\omega_{\text{rot}}}{\omega_c} \right)^2 \right], & \omega_{\text{rot}} < \omega_c, \\ \frac{1}{2} \left(\frac{\omega_c}{\omega_{\text{rot}}} \right)^2, & \omega_{\text{rot}} \geq \omega_c, \end{cases} \quad (13)$$

where Δ_0 is given by the even-odd mass differences of neighboring even-even nuclei, and ω_c is determined by the selfconsistent monopole pairing calculation. The resultant pairing gap parameters are shown in Fig. 4. Now all the mean-field parameters are fixed, and there is no adjustable parameter for the following RPA calculations.

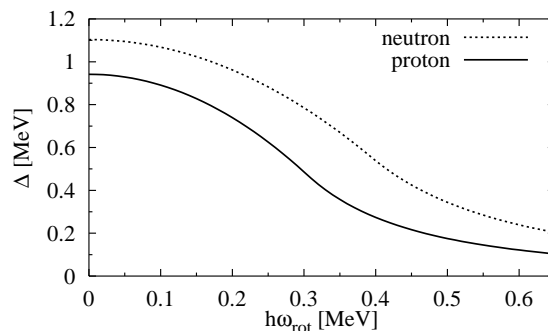


Fig. 4. The neutron and proton gap parameters used in the calculation for the TSD band in ^{163}Lu .

3.2. RPA calculations

Now let us present the results of RPA calculations for the TSD wobbling band in ^{163}Lu , for which most extensive data are available.^{7,16,17} First, Fig. 5 shows the cranking moment of inertia, \mathcal{J}_x in Eq. (12), as a function of the rotation frequency.

^aMore precisely, the expectation values in Eq. (4) is replaced by those with respect to the liquid-drop like sharp cut-off density distribution. Then the γ is determined purely by the geometry of the potential without recourse to actual wave functions.

This inertia is related to the slope of the horizontal rotational band in Fig. 1. Our calculation agrees the trend of experimental data rather well. As for a reference, here and in the following, we also include examples of the particle-rotor model calculations by Hamamoto-Hagemann;⁹ the relevant parameters of the model are $\gamma = 20^\circ$, and $\mathcal{J}_x^{(R)}, \mathcal{J}_y^{(R)}, \mathcal{J}_z^{(R)} = 48, 45, 17 \text{ } \hbar^2 \text{MeV}^{-1}$, respectively. The result of the particle-rotor model is monotonically decreasing, which can be understood by the following approximation valid for a highly aligned quasiparticle band; $\mathcal{J}_x \approx \mathcal{J}_x^{(R)} + j/\omega_{\text{rot}}$, where $j \approx 13/2$ is the maximal alignment of the $\pi i_{13/2}$ orbit.

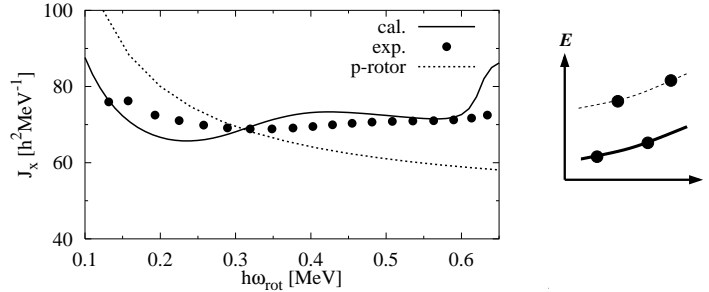


Fig. 5. The moment of inertia, \mathcal{J}_x in Eq. (12) as a function of the rotational frequency in ^{163}Lu . The result of the particle-rotor model is also included as the dotted line with the legend “p-rotor”.

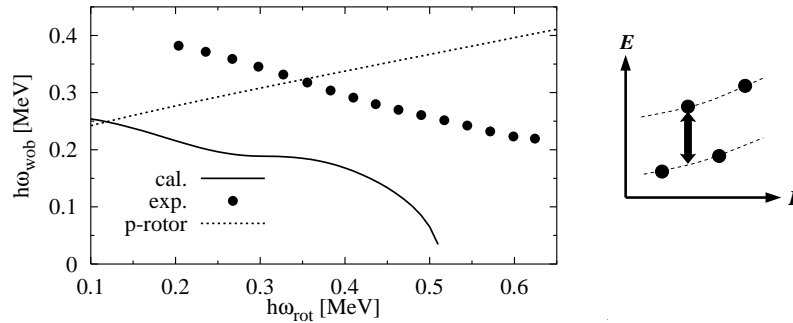


Fig. 6. The excitation energy of the one-phonon wobbling band as a function of the rotational frequency in ^{163}Lu .

Next we show the results of the RPA. We have found that the wobbling-like RPA solution does exist also for the Woods-Saxon mean-field potential; the calculated excitation energy is compared with experimental data in Fig. 6. The solution is stable against the change of mean-field parameters in a reasonable range, so we believe that the existence of the wobbling-like solution has been confirmed. Although the result qualitatively agrees, the calculated excitation energy is smaller than the measured one, and it vanishes at about $\omega_{\text{rot}} = 0.52 \text{ MeV}$. For the excitation energy, the particle-rotor model gives increasing energy as a function ω_{rot} in contrast to the

8 Authors' Names

data. It is, however, difficult to change this general trend as long as the constant moments of inertia of the rotor are used, see Eq. (2).

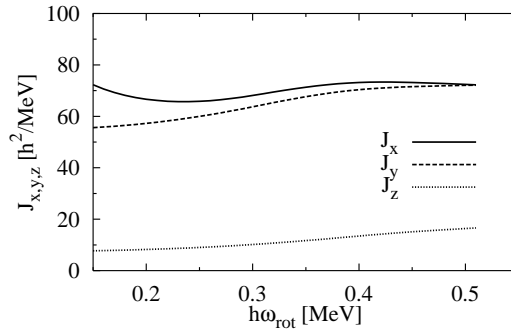


Fig. 7. Three moments of inertia calculated by the Marshalek's theory, Eq. (12), applied to the wobbling-like RPA solution in ^{163}Lu .

In Fig. 7, we show three moments of inertia calculated according to the Marshalek's theory by Eq. (12). Note that they are not the inertia of the rotor, but the total inertia of the system; it is not possible to divide the contribution into the particle and the rotor parts *a priori* in the microscopic calculation. They are not constant but gradually change, which is necessary to understand the decreasing trend of the observed excitation energy.

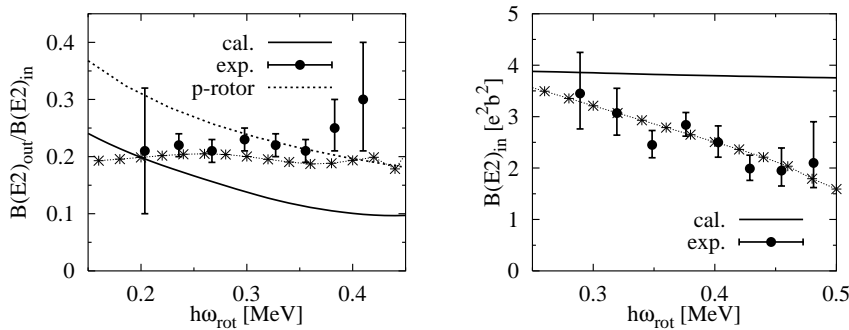


Fig. 8. The out-of-band over in-band $B(E2)$ ratio (left) and the in-band $B(E2)$ (right) as a function of the rotational frequency for the one-phonon wobbling band in ^{163}Lu . The lines connected with star symbols are results of the specific RPA calculation, where the mean-field parameter γ is changed from $\gamma = 12^\circ$ at $\omega_{\text{rot}} = 0.2$ MeV to $\gamma = 22^\circ$ at $\omega_{\text{rot}} = 0.4$ MeV.

Now we come to one of the most important observables, the $B(E2)$, which are depicted in Fig. 8. The measured out-of-band over in-band $B(E2)$ ratio is almost constant (the left part of Fig. 8), but a gradual decrease of the $B(E2)$ ratio as a function of ω_{rot} is expected in the rotor model if the triaxiality parameter γ is kept constant. Both ratios calculated by the RPA approach and by the particle-rotor

model follow this tendency, but our microscopic result is about 60% of the measured value at $\omega_{\text{rot}} \approx 0.3$ MeV, where the particle-rotor model gives correct magnitude. However, the calculated out-of-band $B(E2)$ values are more than 50 Weisskopf units, which is a huge value for a normal RPA solution, and clearly indicates that the obtained solution is not of vibrational but of rotational character ($B(E2)$ values of typical collective vibrations in deformed nuclei are about 10 Weisskopf units at most). The average values of the $B(E2)$ ratio in the particle-rotor model agrees rather well; in fact the parameter $\gamma = 20^\circ$ is chosen for this reason.⁹ Note that our mean-field value is $\gamma = 12^\circ$, and is much smaller; we have checked that almost the same larger value as in the particle-rotor model can be obtained if we use a similar γ value. As for the in-band $B(E2)$, it is just related to the quadrupole moment of the mean-field about the rotating axis (x -axis). The calculated result (the right part of Fig. 8) is almost constant because we have used constant deformation parameters, while the data show a clear tendency to decrease.

As is discussed already, the measured $B(E2)$ strongly suggest that the deformation of the mean-field, especially the triaxiality γ , is changing as a function of the rotational frequency or spin. In the simple rotor model, both the in-band $B(E2)$ and the $B(E2)$ ratio can be estimated approximately as

$$B(E2)_{\text{in}} \approx \frac{15}{32\pi} e^2 \langle \sum_{\pi} (y^2 - z^2) \rangle^2 = \frac{5}{32\pi} e^2 Q_{\pi}^2 \cos^2(\gamma + 30^\circ), \quad (14)$$

$$\frac{B(E2)_{\text{out}}}{B(E2)_{\text{in}}} \approx \frac{2}{I} \left[\frac{(w_z/w_y)^{1/4} \sin(\gamma + 60^\circ) + (w_y/w_z)^{1/4} \sin \gamma}{\cos(\gamma + 30^\circ)} \right]^2, \quad (15)$$

with

$$w_y \equiv 1/\mathcal{J}_z - 1/\mathcal{J}_x, \quad w_z \equiv 1/\mathcal{J}_y - 1/\mathcal{J}_x. \quad (16)$$

The in-band $B(E2)$ depends on both the magnitude of deformation, e.g. ϵ_2 , and the triaxiality γ , while the $B(E2)$ ratio depends only on γ in this approximation. Moreover, these expressions clearly shows that the $B(E2)$ are quite sensitive to the triaxiality parameter γ . The $1/I$ factor in Eq. (15) gives the decreasing trend of the $B(E2)$ ratio if γ and $\mathcal{J}_x, \mathcal{J}_y, \mathcal{J}_z$ are kept constant. Now, can we understand the measured spin dependence of $B(E2)$ by changing the γ parameter? We have tried to play a game by increasing γ linearly from $\gamma = 12^\circ$ at $\omega_{\text{rot}} = 0.2$ MeV to $\gamma = 22^\circ$ at $\omega_{\text{rot}} = 0.4$ MeV, with keeping other parameters unchanged. The results are shown by the lines with star symbols in Fig. 8. Both the $B(E2)$ ratio and the in-band $B(E2)$ nicely agree with data.

4. Summary

We have performed microscopic RPA calculations using the Woods-Saxon potential as a mean-field. We have found that the wobbling-like eigen mode does exist in this calculation. Considering that the similar solutions have been obtained in the previous investigation using the Nilsson potential,^{13,14} we believe that this confirms

the existence of the collective mode, the nuclear wobbling motion, suggested by the macroscopic rotor model.

The calculated excitation energy is smaller than the experimental one by about 100–150 keV. This may suggest that some part of coupling effects to the odd $i_{13/2}$ quasiproton is missing in our calculation. In this respect, Hamamoto-Hagemann has discussed,⁹ by using a simple approximation in the particle-rotor model, that the effect of coupling to the odd particle appears as a constant energy shift to the wobbling energy (2), $\Delta\omega_{\text{wob}} = j/\mathcal{J}_x$, where j is the quasiparticle alignment. Applying this estimate to the case of ^{163}Lu , $j = 13/2$ and $\mathcal{J}_x \approx 70 \hbar^2\text{MeV}^{-1}$, the shift amounts to $\Delta\omega_{\text{wob}} \approx 93$ keV. This fills most part of the energy underestimated in our calculation, although we are not so sure whether such an energy shift can be justified in our microscopic framework: An explicit particle-vibration coupling treatment based on our framework is necessary in order to elucidate this point.

The experimental out-of-band over in-band $B(E2)$ ratio on average suggests larger triaxiality $\gamma \approx 20^\circ$ than the value obtained for TSD minima in the Nilsson Strutinsky calculation, $\gamma \approx 12^\circ$; there is an apparent discrepancy. Note that γ here is defined by Eq. (4), and not the “usual” γ in the Nilsson potential, whose translated value is incidentally about 20° in the case of the TSD bands.

Both the in-band $B(E2)$ and the $B(E2)$ ratio indicate an increase of the triaxial deformation as a function of the rotational frequency or spin. We can obtain nice agreements between the microscopic RPA calculations and the experimental data, if the triaxiality parameter γ is changed linearly, e.g. from $\gamma = 12^\circ$ to 22° . However, the Nilsson-Strutinsky calculation suggests almost constant γ values for TSD minima, and it may be difficult to expect such a large change of γ values. We definitely need more study for quantitative understanding of the observed properties of the nuclear wobbling motion in the Lu region.

References

1. A. Bohr and B. R. Mottelson, *Nuclear Structure Vol.II* (Benjamin, New York, 1975).
2. S. W. Ødegård *et al.*, *Phys. Rev. Lett* **86** (2001) 5866.
3. G. Schönwaßer *et al.*, *Phys. Lett* **B552** (2003), 9.
4. H. Amro *et al.*, *Phys. Lett* **B553** (2003), 197.
5. P. Bringel *et al.*, *Eur. Phys. J.* **A24** (2005), 167.
6. D. R. Jensen *et al.*, *Phys. Rev. Lett* **89** (2002) 142503.
7. A. Görgeň *et al.*, *Phys. Rev.* **C69** (2004) 031301(R).
8. I. Hamamoto, *Phys. Rev.* **C65** (2002) 044305.
9. I. Hamamoto and G. B. Hagemann, *Phys. Rev.* **C67** (2003) 014319.
10. E. R. Marshalek, *Nucl. Phys.* **A331** (1979) 429.
11. Y. R. Shimizu and M. Matsuzaki, *Nucl. Phys.* **A588** (1995) 559.
12. M. Matsuzaki, *Nucl. Phys.* **A509** (1990) 269.
13. M. Matsuzaki, Y. R. Shimizu and K. Matsuyanagi, *Phys. Rev.* **C65** (2002) 041303(R).
14. M. Matsuzaki, Y. R. Shimizu and K. Matsuyanagi, *Phys. Rev.* **C69** (2004) 034325.
15. Y. R. Shimizu and T. Shoji, to be published.
16. D. R. Jensen *et al.*, *Nucl. Phys.* **A703** (2002) 3.
17. D. R. Jensen *et al.*, *Eur. Phys. J.* **A19** (2004) 173.